

Controlling depth of focus in 3D image reconstructions by flexible and adaptive deformation of digital holograms

P. Ferraro,* M. Paturzo, P. Memmolo, and A. Finizio

CNR–Istituto Nazionale di Ottica Applicata and Istituto di Cibernetica, via Campi Flegrei 34,
80078 Pozzuoli (NA), Italy

*Corresponding author: pietro.ferraro@inoa.it

Received June 10, 2009; revised August 16, 2009; accepted August 16, 2009;
posted August 20, 2009 (Doc. ID 112326); published September 9, 2009

We show here that through an adaptive deformation of digital holograms it is possible to manage the depth of focus in 3D imaging reconstruction. Deformation is applied to the original hologram with the aim to put simultaneously in focus, and in one reconstructed image plane, different objects lying at different distances from the hologram plane (i.e., CCD sensor). In the same way, by adapting the deformation it is possible to extend the depth of field having a tilted object entirely in focus. We demonstrate the method in both lensless as well as in microscope configuration. © 2009 Optical Society of America
OCIS codes: 090.1995, 180.3170, 110.0180, 180.6900, 100.3010.

In recent years, digital holography (DH) has revealed its extreme flexibility in 3D imaging. The potential applications of this technology has stimulated efforts to improve the performance of DH such as to improve and control the resolution, to investigate methods for fast and real-time analysis of physical processes, to develop optical configurations with multiple wavelengths, to control and extend the depth of focus, and to compensate aberrations [1–8]. Certainly, one of the key attractive features of DH over other interference microscopy techniques is its intrinsic 3D imaging capability [7–10]. However, for objects having 3D extension or 3D shape, only some portions of the object can be in good focus in each reconstructed plane [11–13]. This is especially true in microscopy, where the need for large magnification causes a harsh squeezing of the depth of field. In classical optical microscopy the problem is solved by mechanically scanning the entire 3D volume with the aim to extract in-focus information from each image plane [14]. In fact, it is possible to build up an extended focus image (EFI), in which all points of the object are in focus. In microscopy, however, the problem of objects changing their shape during the measuring time (i.e., for dynamic events) remains unresolved, because the mechanical scanning takes long time, usually minutes. Among the various approaches a solution to the above problem is the use of coded phase plates [15]. Various viable solutions have been proposed by adopting DH [11,16–21]. In one method the EFI can be built in DH by using amplitude and phase [16], while other methods involve using the angular spectrum of plane waves and coordinates rotations. Nevertheless, a limitation of those methods is the complexity of the numerical computations [17–20]. Increased depth of focus may also be obtained by using diffusion of the images reconstructed along the optical axis [21]. Here we show a method to manage the depth of focus

in DH. The idea behind the proposed approach is very simple. It is based on the fact that the diffraction light distributions in a given plane and the planes in its vicinity along the optical axis are similar and differ only by a magnification constant. An adaptive deformation applied to a digital hologram causes a magnification that allows one to manage and control the depth of focus in the numerical reconstruction process.

Consider a digital hologram of an object recorded at distance d from the CCD. The numerical reconstruction of the object in focus is obtained numerically at distance d from hologram plane by adopting the well-known diffraction Fresnel propagation integral

$$b(x,y) = \frac{1}{i\lambda d} \iint h(\xi,\eta)r(\xi,\eta) \times e^{ikd[1+(x-\xi)^2/2d^2+(y-\eta)^2/2d^2]} d\xi d\eta, \quad (1)$$

where $h(x,y)$ and $r(x,y)$ are the hologram and the reference beam, respectively. If an affine geometric transformation, a deformation, is applied to the original recorded hologram, consisting of a simple stretching described by $[\xi' \eta'] = [\xi \eta 1]T$ through the operator

$$T = \begin{bmatrix} \alpha & 0 \\ 0 & \alpha \\ 0 & 0 \end{bmatrix},$$

we obtain the transformed hologram $h(\xi',\eta') = h(\alpha\xi,\alpha\eta)$. Consequently, the propagation integral changes in

$$\begin{aligned}
 B(x,y,d) &= \frac{1}{i\lambda d} e^{ikd} \int \int h(\alpha\xi, \alpha\eta) e^{ik\alpha^2(x-\xi)^2/2d\alpha^2} e^{ik\alpha^2(y-\eta)^2/2d\alpha^2} d\xi d\eta \\
 &= \frac{1}{i\alpha^2\lambda d} e^{ikd} \int \int h(\xi', \eta') e^{ik(x'-\xi')^2/2D} e^{ik(y'-\eta')^2/2D} d\xi' d\eta' \\
 &= \frac{1}{\alpha^2} b(x', y', D).
 \end{aligned} \tag{2}$$

Such simple stretching applied to the hologram has very interesting consequences on the numerical reconstructions. In fact, from Eq. (2) it is clear that the new hologram reconstructs the object in focus at different distance $D = \alpha^2 d$, while $x' = \alpha x$ and $y' = \alpha y$. We named α the elongation factor.

To show how the stretching operation impacts the numerical reconstructions, we performed different experiments, and the results are reported in Fig. 1. Three different wires were positioned at different distances from the CCD array of 100 mm, 125 mm, and 150 mm, respectively. The optical configuration was in off-axis mode and with a plane reference beam wavefront [$r(x,y) = 1$]. The numerical reconstructions at the above distances give an image in which each wire at a time is in good focus at its recording distance [see Figs. 1(a)–1(c)].

When the hologram $h(x,y)$ is uniformly stretched with an elongation factor along both dimensions (x,y) of $\alpha = 1.22$, the horizontal wire results to be in focus at a different distance $d = 150$ mm [Fig. 1(d)] instead of 100 mm. If $\alpha = 1.1$, the twisted wire with the eyelet is in focus at $d = 150$ mm [Fig. 1(e)] instead of at $d = 125$ mm. Thus the results shown in Fig. 1 demonstrate that the depth of focus can be controlled by means of the uniform stretching of the holograms according to Eq. (2). In case of $\alpha < 1$, the objects are in focus at a shorter distance in respect to the real distance.

These interesting results imply that by an opportune and adaptive deformation, different parts of the 3D scene that are at different depths can be obtained

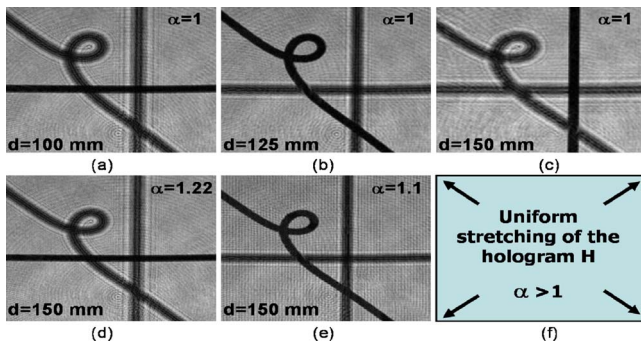


Fig. 1. (Color online) Reconstruction of a digital hologram as recorded (no stretching) at different distances: (a) 100 mm, (b) 125 mm, and (c) 150 mm. For $\alpha = 1.1$ the horizontal wire is in focus at (d) 150 mm, and for $\alpha = 1.22$ the curved wire is in focus at (e) 150 mm. (f) Conceptual draw of the stretching.

in good focus in a single reconstruction, as will be shown below. In fact, the next logical step was to figure out how to deform a hologram with the aim of focusing, on a single reconstruction plane, objects located at different distances from the hologram (i.e., the CCD), but that fall within the same field of view. If we consider a polynomial deformation of $[\xi' \eta'] = [1 \ \xi \ \eta \ \xi^2 \ \eta^2] T$, it can be adapted to the various situations. In our case we used a quadratic deformation such that the operator is

$$T = \begin{bmatrix} 0 & 0 \\ 1 & 0 \\ 0 & 1 \\ 0 & 0 \\ \beta & 0 \\ 0 & \gamma \end{bmatrix}.$$

This time the deformation has been applied only to a portion of the entire hologram. Figures 2(a) and 2(b) respectively show the original recorded hologram and the hologram obtained with the adaptive deformation. The quadratic deformation is very slight, and it has been applied only to the region inside the white ellipse depicted in Fig. 2(b). The deformation is so small that it is difficult to note the difference between the two holograms by a naked eye. To visualize the deformation we show in Fig. 2(c) the beating (moiré) effect by plotting the image given by $|h - h_{\text{def}}|$. We used values for β and γ such that the equivalent average shrinkage in the central part was $\alpha = 0.85$, which allows one to put in focus the wire with the eyelet at $d = 100$ mm. In Fig. 1(c) it is clear that the hologram is unchanged (black area) everywhere except in the region where the deformation was applied. The local shrinkage in the hologram has the effect of moving the eyelet forward, which is now in

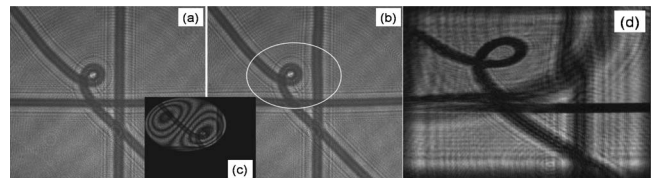


Fig. 2. (a) Hologram as recorded and (b) with local deformation, (c) moiré beating between the two holograms, (d) reconstruction of hologram in (b) with the horizontal wire and the eyelet in focus.

focus together with the horizontal wire [see Fig. 2(d)]. Apart from the obvious distortions in the neighbors, the result shown in Fig. 2(d) demonstrates that two portions of the objects, falling inside of the field of view but at different distances, can be obtained in focus in a single image plane.

One more example is displayed in Fig. 3. In this case the aim of the adaptive deformation is to have in focus in a single image plane horizontal and vertical wires. A quadratic deformation has been applied only along the horizontal direction, i.e., with $\beta=0.0002$ and $\gamma=0$ inside the operator T . When a distortion is applied only along the x axis (anamorphic deformation) it is straightforward to understand that the focus of the horizontal wire is not affected. On the contrary, the diffraction pattern of the vertical wire is magnified by the cylindrical deformation. Figure 3(a) again shows the reconstruction at $d=100$ mm, showing that the horizontal wire is in good focus for the undistorted hologram, while the other two are clearly out of focus. Figure 3(b) shows the reconstruction of the deformed hologram at the very same distance of $d=100$ mm, and in this case both the vertical and the horizontal wires are in focus. It is important to note that the twisted wire experiences different degrees of defocus in the image plane at $d=100$ mm. Essentially we can say that for each portion of the hologram the focus was changed in different way as shown by the parabolic shape of the phase map [see Fig. 3(c)]. It is clear that each portion of the hologram has been stretched differently. Since the quadratic deformation is very small we can approximate it to linear deformation for each small portion of the hologram.

As a final demonstration we show here how to recover the EFI image for a tilted object in a DH microscope. The object is a silicon wafer with the letters "MEMS" written on it. The object was tilted with an angle of 45° in respect to the optical axis of the DH system. The details about the recording of the hologram are reported in [17]. The deformation was applied only along the x axis with $\beta=0.00005$. Figure 4(a) shows the reconstruction of the undistorted hologram at distance of $d=265$ mm [first frame of the video (Media 1) where β was changed in the range 0.0 to 0.00005]. It is important to note that while the portion of the object with the letter "S" in good focus, the remaining is gradually out of focus. Figure 4(b) shows the reconstruction obtained on the quadratic deformed hologram, and it shows that now all the letters "MEMS" are in good focus, demonstrating that

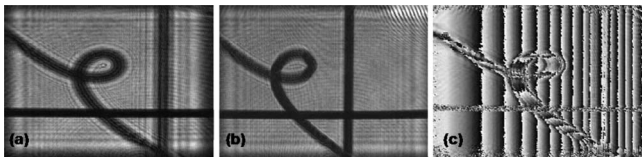


Fig. 3. (a) Reconstruction at 100 mm for the original hologram. (b) Reconstruction of the adaptively deformed hologram. (c) Phase difference.

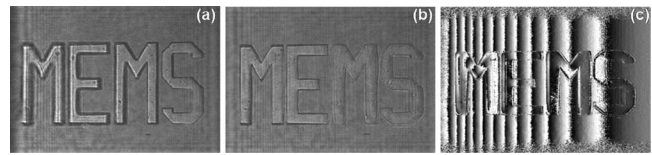


Fig. 4. Quadratic deformation applied along the x axis to an hologram of a tilted object. (a) First frame from the video showing how EFI is get by the adaptively deformation (Media 1). (b) EFI image. (c) Phase difference.

the EFI has been obtained. Figure 4(c) also shows the phase-map difference calculated by subtracting the two holograms, indicating that the defocus tilt has been mainly removed.

In conclusion, we have shown that by means of the hologram's adaptive deformation it is possible to control the reconstruction distance in many situations. The method will open more potentialities in the 3D imaging and microscopy in coherent light by DH.

This research is funded from the European Community's Seventh Framework Programme FP7/2007–2013 under grant agreement 216105.

References

1. *Digital Holography and Three-Dimensional Display: Principles and Applications*, T.-C. Poon, ed., (Springer, 2006).
2. V. Micó, J. García, Z. Zalevsky, and B. Javidi, *Opt. Lett.* **34**, 1492 (2009).
3. Q. Weijuan, Y. Yingjie, C. O. Choo, and A. Asundi, *Opt. Lett.* **34**, 1276 (2009).
4. T. Kim, Y. S. Kim, W. S. Kim, and T.-C. Poon, *Opt. Lett.* **34**, 1231 (2009).
5. M. Kanka, R. Riesenberger, and H. J. Kreuzer, *Opt. Lett.* **34**, 1162 (2009).
6. D. Wang, J. Zhao, F. Zhang, G. Pedrini, and W. Osten, *Appl. Opt.* **47**, D12 (2008).
7. Y. S. Hwang, S.-H. Hong, and B. Javidi, *J. Disp. Technol.* **3**, 64 (2007).
8. Y. Takaki and H. Ohzu, *Appl. Opt.* **39**, 5302 (2000).
9. E. Malkiel, J. N. Abras, and J. Katz, *Meas. Sci. Technol.* **15**, 601 (2004).
10. P. Ferraro, G. Coppola, S. De Nicola, A. Finizio, and G. Pierattini, *Opt. Lett.* **28**, 1257 (2003).
11. M. Antkowiak, N. Callens, C. Yourassowsky, and F. Dubois, *Opt. Lett.* **33**, 1626 (2008).
12. F. Dubois, C. Schockaert, N. Callens, and C. Yourassowsky, *Opt. Express* **14**, 5895 (2006).
13. M. Lieblich and M. Unser, *J. Opt. Soc. Am. A* **21**, 2424 (2004).
14. R. J. Pieper and A. Korpel, *Appl. Opt.* **22**, 1449 (1983).
15. E. R. Dowski, Jr. and W. T. Cathey, *Appl. Opt.* **34**, 1859 (1995).
16. P. Ferraro, S. Grilli, D. Alfieri, S. De Nicola, A. Finizio, G. Pierattini, B. Javidi, G. Coppola, and V. Striano, *Opt. Express* **13**, 6738 (2005).
17. S. De Nicola, A. Finizio, G. Pierattini, P. Ferraro, and D. Alfieri, *Opt. Express* **13**, 9935 (2005).
18. S. J. Jeong and C. K. Hong, *Appl. Opt.* **47**, 3064 (2008).
19. K. Matsushima, *Appl. Opt.* **47**, D110 (2008).
20. C. P. McElhinney, B. M. Hennelly, and T. J. Naughton, *Appl. Opt.* **47**, D71 (2008).
21. C. Do and B. Javidi, *J. Disp. Technol.* **3**, 326 (2007).